An Efficient Equilibrium Optimizer for Parameters Identification of Photovoltaic Modules

Essam H. Houssein[1]**, Gamela Nageh Zaki**[1]**, Mohamed Abd Elaziz**[2]**, and Eman M.G. Younis**[1]

[1]**Faculty of Computers and Information, Minia University, Minia, Egypt.**
[2]**Department of Mathematics, Faculty of Science, Zagazig University, Zagazig, Egypt.**

Corresponding author:
Gamela Nageh Zaki[1]

Email address: gamela.nageh@mu.edu.eg

ABSTRACT

The use of solar photovoltaic systems (PVs) is increasing as a clean and affordable source of electric energy. The Pv cell is the main component of the PV system. To improve the performance, control, and evaluation of the PV system, it is necessary to provide accurate design and to define the intrinsic parameters of the solar cells. There are many methods for optimizing the parameters of the solar cells. The first class of methods is called the analytical methods that provide the model parameters using datasheet information or I–V curve data. The second class of methods is the optimization-based methods that define the problem as an optimization problem. The optimization problem objective is to minimize the error metrics and it is solved using metaheuristic optimization algorithms. The third class of methods is composed of a hybrid of both the analytical and the metaheuristic approaches, some parameters are computed by the analytical approach and the rest are found using metaheuristic optimization algorithms. Research in this area faces two challenges; 1) finding an optimal model for the parameters of the solar cells and 2) the lack of data about the photovoltaic cells.

This paper proposes an optimization-based algorithm for accurately estimating the parameters of solar cells. It is using the Improved Equilibrium optimizer Algorithm (IEO). This algorithm is improved using the Opposition Based Learning (OBL) at the initialization phase of EO to improve its population diversity in the search space. Opposition-based Learning (OBL) is a new concept in machine learning inspired by the opposite relationship among entities. There are two common models for solar cells; the single diode model (SDM) and double diode model (DDM) have been used to demonstrate the capabilities of IEO in estimating the parameters of solar cells. The proposed methodology can find accurate solutions while reducing the computational cost. Compared to other existing techniques, the proposed algorithm yields less mean absolute error. The results were compared with seven optimization algorithms using data of different solar cells and PV panels.The experimental results revealed that IEO is superior to the most competitive algorithms in terms of the accuracy of the final solutions.

INTRODUCTION

A major drawback of the use of fossil fuel is its negative environmental effects; therefore, alternative renewable energy sources (RESs) are used as an alternative clean and affordable energy source. There are seven types of RESs namely, biomass López et al. (2008), geothermal Houssein (2019), wind Osama et al. (2017), solar Hocaoğlu (2011); Munshi and Yasser (2017), hydroelectric Bagher et al. (2015), hydrogen Dunn (2002), and tide Egbert and Ray (2000). Solar energy is considered one of the most important sources of renewable energy, as the sun plays a significant role in it's generation. A PV system uses solar cells (SCs) to convert the sunlight into electricity AbdElminaam et al. (2021).

PV SCs are a type of RES that is clean (i.e., generates no pollution), has a long life, has a simple design and easy to install. However, solar energy has several drawbacks compared with other RES. The main disadvantages of PV solar energy systems are the high initial exploitation and low capacity of SCs

Abbreviations

PV	Photovoltaic	IEO	Improved Equilibrium optimizer Algorithm
EO	Equilibrium optimizer Algorithm	OBL	Opposition Based Learning
SDM	single diode model	DDM	double diode model
RESs	renewable energy sources	SCs	system uses solar cells
V_{oc}	open circuit voltage	Vmpp	voltage at the point of maximum power
I_{mpp}	current at the point of maximum power	I_{sc}	short-circuit current
P_{mpp}	maximum power	Kv	voltage temperature coefficients
Ki	current temperature coefficients	I_o	the reverse saturation current
Ipv	photogenerated current	a	non-physical ideality factor of the diode
R_p	shunt resistance	R_s	series resistant
GA	a genetic algorithm	PSO	particle swarm optimization
SA	simulated annealing	GWO	gray wolf optimizer
FPA	flower pollination algorithm	MSSO	simplified swarm optimization algorithm
I_D	The diode current	$I_{o,cell}$	The reverse saturation current of the diode
N_c	represents the number of cells	K	Boltzmann constant
q	charge of an electron	T	The temperature (in Kelvin)
$C_i^{initial}$	The initial condensation of the i_{th} particle	C_{max}	The maximum of the dimensions
C_{min}	The minimum of the dimensions	n	the particle number representing a population
G	key expression of the proposal technique	WOA	whale optimizer algorithm
SCA	since-cosine algorithm	MVO	Multi-Verse Optimizer
ABC	artificial bee colony	WDO	Wind Driven Optimization
SCE	Sister chromatid exchange	ImCSA	improved cuckoo search algorithm
ISCA	Interview Schedule For Children and Adolescents	SMA	Superior Mesenteric artery
COA	Coyote optimization algorithm	TLO	Teaching-learning-based optimization

46   Navabi et al. (2015). An open research topic is optimizing the efficiency of SCs. Because PV modules are
47   installed outdoors, the weather conditions affect the generated energy, which results in a high maintenance
48   cost and difficulty in control.

49   PV modules contain SCs, which consist of a semiconductor of monocrystalline material (KC200GT)
50   Park et al. (2014), monocrystalline (SM55) Salam et al. (2010), and thin film (ST40) Alam et al. (2015a).
51   The global settings of a SC depend on a circuit to examine the performance of the cell under various
52   conditions, such as temperature and solar irradiance. A SC can be described by the following two
53   popular models: the single-diode model (SDM) and the double-diode model (DDM) Lim et al. (2015);
54   Humada et al. (2016); Ismaeel et al. (2021). The SDM is similar to the DDM, and the variation in cellular
55   performance is imperceptible. The SDM is more common than the DDM. The SDM model includes five
56   unknown parameters, while the DDM has seven unknown parameters. Accurate determination of the
57   unknown variables plays an important role in optimizing the SC and it's internal parameters.

58   The PV module manufacturer's data sheet contains the parameters of the open circuit voltage (Voc),
59   voltage and current at the point of maximum power (Vmpp and Impp), short-circuit current (Isc), maximum
60   power (Pmpp), voltage temperature and current temperature coefficients (Kv and Ki). These parameters
61   can also be obtained experimentally. The SDM, however, requires other parameters, such as the reverse
62   saturation current (Io), photogenerated current (Ipv), nonphysical ideality factor of the diode (a), shunt
63   resistance (Rp), and series resistance (Rs). However, these parameters are not provided in the data sheet.
64   Therefore, determining these parameters is a major research challenge.

65   There are three types of approaches for solving the parameter estimation problem: traditional methods
66   (analytical methods) Easwarakhanthan et al. (1986), metaheuristic methods AlRashidi et al. (2011) and
67   hybrid methods. Traditional methods use a modified nonlinear least squares estimation approach based on
68   Newton's method. Traditional approaches depend on the starting point of the iterative method, which
69   is a key problem. As a result, these methods tend to be trapped in local solutions. An example of this
70   type of techniques is presented in Chan et al. (1986). Several features, such as convexity, continuity,
71   and differentiability, are required for usability. The drawbacks of these methods include high demand
72   of computational resources, sensitivity to initial conditions, and the tendency to provide sub-optimal
73   solutions.

74   Unlike conventional methods, metaheuristic approaches have been proposed to increase the probability
75   of obtaining the global solution in a reasonable time. In the literature, the problem of determining the
76   parameters of the SC has been solved using genetic algorithms (GA) Ismail et al. (2013), particle swarm
77   optimization (PSO) Wei et al. (2011a), and simulated annealing (SA) El-Naggar et al. (2012a). Although
78   these metaheuristic algorithms produce better solutions than conventional algorithms, they have some
79   limitations Dai et al. (2009). The third approach for solving this problem is using hybrid methods which

use a combination of the analytical and the metaheuristic approaches. A review of the methods of the
parameter estimation of the SCs is presented in Oliva et al. (2019).

Recently, researchers have used metaheuristic algorithms to extract the optimal parameters of PV
systems Oliva et al. (2019). These algorithms include the bird -mating optimizer Askarzadeh and
Rezazadeh (2013c), artificial immune system Jacob et al. (2015), repaired adaptive differential evolution
Gong and Cai (2013), pattern search AlHajri et al. (2012), harmony search-based algorithms Askarzadeh
and Rezazadeh (2012), SA El-Naggar et al. (2012b), chaos particle swarm algorithm Wei et al. (2011b),
artificial bee colony Askarzadeh and Rezazadeh (2013a), the mutative-scale parallel chaos optimization
algorithm Yuan et al. (2014), adaptive differential evolution Chellaswamy and Ramesh (2016), gray wolf
optimizer (GWO) Rodríguez and Murillo (2017), mine blast algorithm El-Fergany (2015), improved
shuffled complex evolution algorithm Gao et al. (2018a), direct search optimization algorithm Osheba
et al. (2017), evaporation-rate-based water cycle algorithm Gotmare et al. (2017), Tabu search Siddiqui
and Abido (2013), and chaos PSO Wei et al. (2011c).

An interesting approach to solve the problem of solar PV parameter estimation is based on the flower
pollination algorithm (FPA) Alam et al. (2015b). The FPA mimics flower pollination behavior. However,
its results are inaccurate. The multi-verse optimizer has also been used to extract the parameters of the
PV system. But, this algorithm also generates results far from the optimal solution Ali et al. (2016).
An optimization algorithm for artificial swarms of bees identifies parameters of the SC models and is
inspired by the intelligent behaviors of the bees, such as collecting and processing nectar Askarzadeh and
Rezazadeh (2013b). The simplified swarm optimization algorithm (*MSSO*) has been applied to both the
SDM and DDM to minimize the square error between the experimental and calculated data. However, this
minimization was not efficient $9.8607E^{-04}$ Lin et al. (2017a). The improved chaotic whale optimization
algorithm has also been used to estimate the parameters of the PV. But, it is complex and difficult to apply
Oliva et al. (2017b). The most recent typologies in the literature are listed in Table 1.

The above methods use metaheuristic algorithms that require large computational time and lead to high
error rate between the experimental and the calculated data. Therefore, this work proposes an efficient
algorithm called the improved equilibrium optimizer (IEO) algorithm to estimate the optimal parameters
of the PV system. IEO was validated by comparing its results with those of a mathematical method and
other approaches. Using the IEO, the minimum error between the estimated and the experimental data and
the minimum convergence time for the optimal parameters and the best curve fit (I-V) was obtained. An
accurate PV model based on IEO algorithm can play an important role in increasing the overall efficiency
of a PV system. It guarantees the optimal use of the available solar energy, which results in reducing the
costs of the PV system. To the best of our knowledge, the IEO is a new optimization algorithm whose
potential has not yet been extensively applied in real problems. The motivation of this paper is to propose
a parameter estimation technique for efficiently and accurately extracting the parameters of the SCs and
PV modules. The major contributions of this work are as follows:

1. Proposing the Improved Equilibrium optimizer (IEO) algorithm, which is inspired by the control,
   volume, mass, and balance models for estimating the Photovoltaic (PV) parameters.

2. IEO algorithm proved that it can obtain the optimal value of the PV variables of single and double
   diode models.

3. Comparing the IEO with other metaheuristic algorithms the results show that IEO provided smaller
   errors between the calculated values and the actual values.

The remainder of this paper is organized as follows: Section 1 offers a depiction of the mathematical
model of the PV cell/module. Equilibrium optimizer (EO) and Improved Equilibrium optimizer (IEO) are
presented in sections 2 and 3, respectively. The modified objective function is introduced in Section 4. In
Sections 5 and 6 analysis and Comparative study of the proposed algorithm with other meta-heuristics
algorithms are provided. Finally, the conclusions and future work are presented in Section 7.

1 MATHEMATICAL MODEL OF PHOTOVOLTAIC CELL/MODULE

This section presents the mathematical model of the PV unit Biswas et al. (2019) that can be obtained
by the SDM El-Arini et al. (2013) and DDM Chin et al. (2011). Fig. 1 displays the equipollent circuit
diagram of a typical PV cell. The current (I) of this cell is as follows:

$$I = I_{PV,Cell} - I_D \qquad (1)$$

Table 1. Summary of the previous related research.

Year	Method	RMSE
2017	MSSO Lin et al. (2017b)	SDM: $9.8607E^{-04}$ DDM: $9.8281E^{-04}\%$
2017	ABC with chaotic maps Oliva et al. (2017c)	SDM: 9.8602×10^{-04} DDM: 9.8262×10^{-04}
2017	WDO Derick et al. (2017)	SDM: 0.00084 DDM: 0.00106
2017	WOA with chaotic maps Oliva et al. (2017a)	SDM: $9.8602 \times 10^{-04}\%$ DDM: 9.8272×10^{-04}
2018	SCE with a complex evolution strategy Gao et al. (2018b)	SDM: 9.860219×10^{-04} DDM: 9.824849×10^{-04}
2018	WDO Mathew et al. (2017)	DDM: 0.127
2018	ImCSA Kang et al. (2018)	SDM: $9.8602E^{-04}$ DDM: $9.8249E^{-04}$
2019	TLO Li et al. (2019)	SDM: $9.8609E^{-04}$ DDM: $9.8612E^{-04}$
2019	ISCA Chen et al. (2019)	SDM: $9.8602E^{-04}$ DDM: $9.8237E^{-04}$
2020	SMA Kumar et al. (2020)	SDM: $9.8582E^{-04}$ DDM: $9.8148E^{-04}$
2020	COA Diab et al. (2020)	SDM: $7.7547E^{-04}$ DDM: $7.6480E^{-04}$
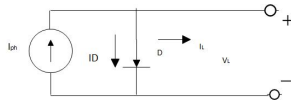
Figure 1. Equivalent circuit of an ideal photovoltaic (PV) cell.
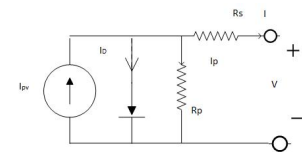
Figure 2. Single-diode model of photovoltaic (PV) cell.
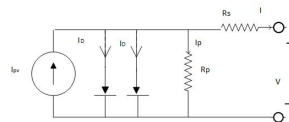
Figure 3. Double diode model of the PV cell.

where, $I_{PV,Cell}$ is the PV current and I_D is the diode current.

$$I_D = I_{O,Cell}[exp(\frac{qV}{aKT}) - 1] \tag{2}$$

where, $I_{O,Cell}$ is the reverse saturation current of the diode, q ($1.60217646 \times 10^{-19}(coulomb)$) is the charge of an electron, k ($1.38064852 \times 10^{-23}Joules/Kelvin$) is the Boltzmann constant, T is the temperature (in Kelvin) of the diode junction, and a is the ideal factor of the diode. Therefore, Eq. 1 can be rewritten to obtain the I-V characteristic of a typical cell as follows:

$$I = I_{PV,Cell} - I_{O,Cell}[exp(\frac{qV}{aKT}) - 1] \tag{3}$$

PV cells can be linked either in parallel or in series to form a PV system. Here, N_c represents the number of cells that are linked in series.

Single diode model

In the SDM, five unknown parameters must be obtained. These parameters are the photon current (I_{pv}), reverse saturation current of the diode (I_o), the ideality factor (a), and the series and parallel resistances (R_s and R_p). Fig. 2 presents the SDM of a PV cell with N_C series-connected cells.

Therefore, the $I - V$ characteristics of the SDM of the PV are represented as:

$$I = I_{PV} - I_O[exp\frac{q(V+R_SI)}{aKN_CT} - 1] - \frac{V+R_SI}{R_S} \tag{4}$$

4/17

At the point of the open circuit, we find that $(V = V_{OC})$ and $(I = 0)$ (opinion); thereafter, from Eq.(4), we obtain;

$$0 = I_{PV} - I_O[exp(\frac{qV_{OC}}{aKN_CT}) - 1] - \frac{V_{OC}}{R_P} \tag{5}$$

$$Thus, \quad I_{PV} = I_O[exp(\frac{qV_{OC}}{aKN_CT}) - 1] - \frac{V_{OC}}{R_P} \tag{6}$$

At the point of the short circuit $(I = I_{SC})$ and $(V = 0)$ (opinion); thereafter, from Eq.(4) we obtain;

$$I_{SC} = I_{PV} - I_O[exp(\frac{qR_SI_{SC}}{aKN_CT}) - 1] - \frac{R_SI_{SC}}{R_P} \tag{7}$$

$$Therefore, \quad I_{PV} = I_{SC} + I_O[exp(\frac{qR_SI_{SC}}{aKN_CT}) - 1] - \frac{R_SI_{SC}}{R_P} \tag{8}$$

From Eq. (6) and Eq. (8) we have;

$$I_O = \frac{I_{SC} + \frac{R_SI_{SC}}{R_P} - \frac{V_{OC}}{R_P}}{exp(\frac{qV_{OC}}{aKN_CT}) - exp(\frac{qR_SI_{SC}}{aKN_CT})} \tag{9}$$

Substituting Eq. (9) into Eq. (6) yields;

$$I_{PV} = \frac{(I_{SC} + \frac{R_SI_{SC}}{R_P} - \frac{V_{OC}}{R_P})[exp(\frac{qV_{OC}}{aKN_CT} - 1]}{exp(\frac{qV_{OC}}{aKN_CT}) - exp(\frac{qR_SI_{SC}}{aKN_CT})} \tag{10}$$

At the maximum power point $(V = V_{MPP})$ and $(I = I_{MPP})$ (say), fromEq. (4) we have;

$$I_{MPP} = I_{PV} - I_O[exp\frac{q(V_{MPP}+R_SI_{MPP})}{aKN_CT} - 1] - \frac{V_{MPP}+R_SI_{MPP}}{R_P} \tag{11}$$

Double-diode model

In the DDM in Fig. 3, seven unknown parameters must be obtained. These parameters are the photon current (I_{pv}), reverse saturation current of the first diode (I_{O1}), reverse saturation current of second diode (I_{O2}), ideality factors of the first and second diodes (a_1) and a_2, and the PV cell series and parallel resistances $(R_S$ and $R_P)$. Therefore, the I-V characteristics of the DDM are as follows:

$$I = I_{PV} - I_{D1} - I_{D2} - \frac{V+R_sI}{R_P} \tag{12}$$

$$i.e. \quad I = I_{PV} - I_{O1}[exp\frac{q(V+R_SI)}{a_1KN_CT} - 1] - I_{O2}[exp\frac{q(V+R_SI)}{a_2KN_CT} - 1] - \frac{V+R_SI}{R_P} \tag{13}$$

At the point of the open circuit, $I = 0$ and $V = V_{OC}$; thus, from Eq.13 we obtain;

$$0 = I_{PV} - I_{O1}[exp\frac{q(V+R_SI)}{a_1KN_CT} - 1] - I_{O2}[exp\frac{q(V+R_SI)}{a_2KN_CT} - 1] - \frac{V_{OC}}{R_S} \tag{14}$$

$$Therefore, \quad I_{PV} = O1[exp\frac{q(V+R_SI)}{a_1KN_CT} - 1] - I_{O2}[exp\frac{q(V+R_SI)}{a_2KN_CT} - 1] - \frac{V_{OC}}{R_S} \tag{15}$$

At the point of the short circuit, $V = 0$ and $I = I_{SC}$; thus, from Eq.(13) we obtain;

$$I_{SC} = I_{PV} - I_{O1}[exp(\frac{qR_SI_{SC}}{a_1kN_CT}) - 1] - I_{O2}[exp(\frac{qR_SI_{SC}}{a_2kN_CT}) - 1] - \frac{R_SI_{SC}}{R_P} \tag{16}$$

$$Therefore, \quad I_{PV} = I - SC + I_{O1}[exp(\frac{qR_SI_{SC}}{a_1kN_CT}) - 1] + I_{O2}[exp(\frac{qR_SI_{SC}}{a_2kN_CT}) - 1] + \frac{R_SI_{SC}}{R_P} \tag{17}$$

From Eq. (15) and Eq. (17) we have;

$$I_{O2} = \frac{I_{SC} + \frac{R_SI_{SC}}{R_P} - \frac{V_{OC}}{R_P} - I_{O1}[exp(\frac{qV_{OC}}{a_1kN_CT}) - exp(\frac{qR_SI_{SC}}{a_1kN_CT})]}{exp(\frac{qV_{OC}}{a_2kN_CT}) - exp(\frac{qR_SI_{SC}}{a_2kN_CT})} \tag{18}$$

Substituting Eq. (18) into Eq. (15) yields;

$$I_{PV} = I_{O1}[exp(\frac{qR_SI_{SC}}{a_1kN_CT}) - 1] + \frac{I_{SC} + \frac{R_SI_{SC}}{R_P} - \frac{V_{OC}}{R_P} - I_{O1}[exp(\frac{qV_{OC}}{a_1kN_CT}) - exp(\frac{qR_SI_{SC}}{a_1kN_CT})]}{[exp(\frac{qV_{OC}}{a_2kN_CT}) - exp(\frac{qR_SI_{SC}}{a_2kN_CT})][exp(\frac{qV_{OC}}{a_2kN_CT}) - 1]^{-1}} + \frac{V_{OC}}{R_P} \tag{19}$$

At the maximum power point, $V = V_{MPP}$ and $I = I_{MPP}$ (say); then, from Eq. (13) we obtain;

$$I_{MPP} = I_{PV} - I_{O1}[exp\frac{q(V_{MPP}+R_SI_{MPP})}{a_1kN_CT} - 1] - I_{O2}[exp\frac{q(V_{MPP}+R_SI_{MPP})}{a_2kN_CT} - 1] - \frac{V_{MPP}+R_SI_{MPP}}{R_P} \tag{20}$$

2 EQUILIBRIUM OPTIMIZER (EO) ALGORITHM

In this section, we discuss the exploratory and exploitative phases of EO, inspired by the general mass balance equation for a control volume Faramarzi et al. (2020).

Initialization and evaluation of functions

Like many metaheuristic algorithms, the EO uses the initial population for beginning the optimization process. The processing in this method is divided into two phases: the first phase is the "teacher phase," which means learning from the teacher, and the second phase is the "learner phase," which means learning by interacting with other learners.These phases are consecutively iterated to produce better results until convergence is achieved. In EO, each particle (solution) with its concentration (position) acts as a search agent. Some solutions and their dimensions experience mutation, defined by a function, and selected by a parameter such as mutation probability and percentage The initial concentration is structured according to the particle number and dimensions, with normal initialization appearing as follows:

$$C_i^{initial} = C_{min} + rand_i(C_{max} - C_{min}) \qquad i = 1, 2, \ldots, n \tag{21}$$

$C_i^{initial}$ is the initial condensation of the ith particle, C_{max} and C_{min} are the maximum and minimum of the dimensions, respectively, and $rand_i$ is in the domain [0,1] so that n is the particle number representing a population. Particles are examined and thereafter classified as candidates.

Equilibrium pool and candidates C_{eq}

The equilibrium case takes into consideration the last case of convergence of the algorithm, which should be the global optimum. At the beginning of the optimization algorithm, the equilibrium state is unknown, and it is only determined by the candidate that the equilibrium data creates a research model for particles. Depending on various factors, these candidates are identified, four particles specific to the optimization, and the condensation of others particle is the arithmetic mean of those. The number of candidates is random and depends on the nature of the problem. For example, the GWO uses the three best candidates (β, γ and α wolves) to change place with other wolves. More than four candidates can positively impact these five particles and are used as candidates for balancing to build a vector that is the equilibrium set in Eq.(22):

$$\vec{C}_{eq,pool} = \{\vec{C}_{eq(1)}, \vec{C}_{eq(2)}, \vec{C}_{eq(3)}, \vec{C}_{eq(ave)}\} \tag{22}$$

Every particle at every repetition changes its condensation to select randomly from the candidate's selection with the same prospect.

Exponential term (F)

The following exponential expression (F) contributes to the rule of changing condensation. A precise introduction of this expression leads to the balance of exploration and exploitation. The fluctuation range can change over time in an actual dominance volume, and should be a vector in the domain of [0,1] as in Eq.(23):

$$\vec{F} = e^{-\vec{\lambda}(t-t_o)} \tag{23}$$

Thus, time, t, known as the task of iteration (*Iter*), reduces the repetition number of Eq.(24):

$$t = (1 - \frac{Iter}{Max\_iter})^{(a_2 \frac{Iter}{Max\_iter})} \tag{24}$$

where, Max_iter and $Iter$ represent the maximum number of iterations and the current, respectively, and a2 is a constant utilized to administer the capacity of use. To warranty concourse and improve the exploration and exploitation capacity of the EO, this is given as;

$$\vec{t}_o = \frac{1}{\vec{\lambda}} \ln(-a_1 sign(\vec{r} - 0.5)[1 - e^{-\vec{\lambda}t}]) + t \tag{25}$$

Here, a_1 is a constant that controls the exploration capacity, while a_2 is a constant that controls the exploitation ability. Furthermore, r is a vector in the range [0–1] selected randomly. $Sign(r - 0.5)$ impacts the direction of exploration and exploitation. a_1 and a_2 are 2 and 1, respectively, for all problems. The derived form of Eq. (23) with the substitution Eq.(25) is represented in Eq.(26) as follows:

$$\vec{F} = a_1 sign(\vec{r} - 0.5)[e^{-\vec{\lambda}t} - 1] \tag{26}$$

146 **Generation rate** (G)

G is another key expression of the proposed technique for providing the precise solution by enhancing exploitation. For example, a multipurpose model that characterizes G as the top-order exponential decomposition operation is as follows:

$$\vec{G} = \vec{G}_o e^{-\vec{K}(t-t_o)} \tag{27}$$

where, G_o is the initial value and k represents the attenuation constant. For restricting the random variables, suppose that $K = \lambda$, and utilize the formerly derived exponential expression. The conclusive set of G is as follows:

$$\vec{G} = \vec{G}_o e^{-\vec{\lambda}(t-t_o)} = \vec{G}_o \vec{F} \tag{28}$$

$$where: \qquad \vec{G}_o = \vec{GCP}(\vec{C}_{eq} - \vec{\lambda}\vec{C}) \tag{29}$$

$$\vec{GCP} = \begin{cases} 0.5 r_1 & r_2 \geq GP \\ 0 & r_2 < GP \end{cases} \tag{30}$$

Here, GCP is the control parameter for the generation rate that contains the potential of the generation expression assistance for the update procedure. In addition, r_1 and r_2 are random vectors in [0,1]. Finally, the EO update rule is as in Eq. (31):

$$\vec{C} = \vec{C}_{eq} + (\vec{C} - \vec{C}_{eq}).\vec{F} + \frac{\vec{G}}{\vec{\lambda}V}(1 - \vec{F}) \tag{31}$$

147 where, F is presented in Eq. (26), and V is a unit. To summarize all the aforementioned steps, a framework
148 for EO is drawn in Fig. 4. Fig. It displays a conceptual sketch of the cooperation of all candidates
149 for balance in a set of sample particles and how they sequentially affect the concentration update in
150 the proposed algorithm. Since the topological positions of the equilibrium candidates are different in
151 the initial iteration, and the exponential term generates large random numbers, this step-by-step update
152 process helps particles that cover the entire area of the research. In the latter case, the opposite scenario
153 occurs iterations when candidates circle the sweet stop with similar attitudes. To this sometimes the
154 exponential term generates small random numbers, which helps in refining the solutions. Providing
155 smaller step sizes. This concept can also be extended to higher dimensions such as hyperspace in which
156 the concentration is updated with the movement of the particle in n-dimensional space.

157   The EO algorithm has been tested for three known engineering design problems. A simple method of
158 constraint management, the static penalty, is used here to punish the objective function with high score
159 when constraints are violated at any level from their defined limits. The penalty coefficient must be large
160 enough to correctly punish the objective function under the conditions of equality/inequality. Note that all
161 technical test problems ran with the same number of iterations (500) and particles (30) according to the
162 math functions described above.

3 IMPROVED EQUILIBRIUM OPTIMIZER (IEO) ALGORITHM

164 We improved the Equilibrium optimizer algorithm to give the best result that is closest to the global
165 optimum. The improvement has been done by using opposition-based learning (OBL). The Equilibrium
166 optimizer algorithm with OBL gave better values to the unknown parameters of PV than Equilibrium
167 optimizer without improvement.

3.1 Opposition based learning (OBL)

169 The basic concept of Opposition-Based Learning (OBL) was originally introduced by Tizhoosh, 2005.
170 The basic aim of this algorithm is optimization, to find the best candidate solution, the simultaneous
171 consideration of an estimate and its corresponding opposite estimate which is closer to the global optimum.
172 This has been achieved in a very short time and it has been used in various areas of soft computing.
173 Opposition-based Learning (OBL), which has been used for improving convergence of the metaheuristic
174 techniques for finding the global solution of the optimization problem. OBL theory has been applied
175 to solve many real-world problems such as optimization and estimation of photovoltaic parameters. In
176 general, any metaheuristic algorithm begins with creating an initial population as an attempt for finding
177 the optimum solution(s), these initial solutions are generated randomly or based on a specific search
178 range.
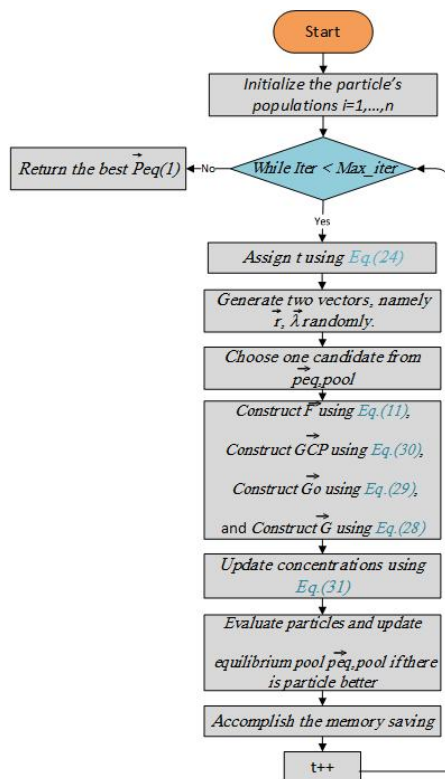
Figure 4. A flowchart of the equilibrium optimizer (EO) algorithm.
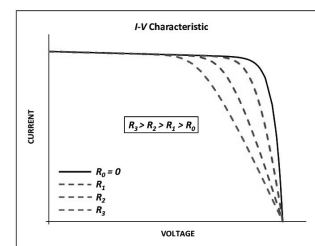
Figure 5. Effects of the series resistance on the I-V characteristic.

3.1.1 Opposite number

x is defined as a real number over the domain $x \in [lb, ub]$. The opposite of x is represented by $\bar{x}$ and is identified as :

$$\bar{x} = ub + lb - x \tag{32}$$

where ub and lb are the upper and lower bound of the search space. Eq. 32 can be generalized to be used in a search area with multi-dimensions. Therefore, to generalize it, every search-agent position and its opposite position will be introduced as the following :

x = $[x_1, x_2, x_3, x_4, ..., x_D]$ and $\bar{x} = [\bar{x}_1, \bar{x}_2, \bar{x}_3, \bar{x}_4, ..., \bar{x}_D]$ The values of all parameters in $\bar{x}$ will be estimated as :

$$\bar{x}_j = ub_j + lb_j - x_j \qquad where \, j = 1, 2, 3, ..., D \tag{33}$$

3.1.2 Opposition based learning

In this optimization strategy if the fitness function $f(\bar{x})$ of the opposite solution is better than fitness function $f(x)$ of its original solution x, then $x = \bar{x}$; otherwise $x = x$.

4 OBJECTIVE FUNCTION

The major purpose of estimating the parameters for SDM and DDM is to detect the Parameter values that reduce the differences between the measured and calculated current that can be determined with an objective function. Table 2 presents details about the parameters that are optimized by IEO technique. The parameters were computed depending on the special connections that were discussed in Section 1 for the SDM and DDM. For the DDM, $(a_1), (a_2), (R_S), (R_P)$ and (I_{O1}) are optimized. (I_{pv}) and (I_{o2}) are computed by variables that are optimized utilizing the relationship discussed in Section 1. Metaheuristic algorithms are necessary to minimize errors at three points (open circuit $[0, V_{OC}]$, short circuit $[I_{SC}, 0]$, and points of maximum power $[I_{MPP}, V_{MPP}]$). For the SDM, the error at the open circuit (from Eq. 6) is;

$$err_{OC} = I_O[exp(\frac{qV_{OC}}{akN_CT}) - 1] + \frac{V_{OC}}{R_p} - I_{PV} \tag{34}$$

Table 2. Optimized parameters for the single-diode and double-diode model.

Models	Optimized variables	Calculated variables
Single-diode model	a, Rs, Rp	Io (Eq.(9)) and Ipv (Eq.(10))
Double-diode model	a1, a2, Rs, Rp,Io1	Io2 (Eq.(18)) and Ipv(Eq.(19))

The error at the short circuit (from Eq. 8) is;

$$err_{SC} = I_{SC} + I_O[exp(\frac{qR_SI_{SC}}{akN_CT}) - 1] + \frac{R_SI_{SC}}{R_P} - I_{PV} \tag{35}$$

The error at the maximum power point (from Eq.11) is;

$$err_{MPP} = I_{PV} - I_O[exp(\frac{q(V_{MPP}+R_SI_{MPP})}{akN_CT}) - 1] - \frac{V_{MPP}+R_SI_{MPP}}{R_P} - I_{MPP} \tag{36}$$

The same applies for the error values of the DDM, which can be derived using Eqs.(15), (17) and (20) at these three points. The goal of optimization is considered the sum of the quadratic errors:

$$ERR = err_{OC}^2 + err_{SC}^2 + err_{MPP}^2 \tag{37}$$

5 SIMULATION RESULTS AND ANALYSIS

To verify the accuracy, reliability, and robustness of the IEO algorithm, we evaluate the performance of the IEO algorithm for estimating the parameters of a PV cell, namely, the SDM and DDM. For every SDM and DDM for all SC types (polycrystalline, thin-film, and monocrystalline), the IEO were run separately 30 times. A MATLAB model was developed for testing the algorithms presented above. In addition, variables such as open-circuit voltage (V_{OC}), short circuit current (I_{SC}), maximum power point voltage (V_{MP}), maximum power point current (I_{MP}), voltage temperature coefficient (K_V), and current temperature coefficient (K_i) were provided in the manufacturer's data sheet. All characteristics passed through three specified points are illustrated in Table 3 as follows: Open circuit:$V = V_{OC} = 32.9$ volt, $I = 0$ amp; Short circuit: $V = 0$ volt,$I = I_{SC} = 8.21$ amp; Maximum power: $V = V_{MPP} = 26.3$ volt, $I = I_{MPP} = 7.61$ amp. The algorithm was run on the MATLAB R2010a platform on a system with 4 GB RAM and an i3 processor. Improved code of equilibrium optimization using opposition-based learning is available in supplemental Source_Code file. Code to generated datasets used to test the code is available inside supplemental Datasets file. After improved Equilibrium optimization by opposition-based learning, we found the algorithm found smaller error than before.

Numerical data

This study examined three types of SCs: polycrystalline, thin-film, and monocrystalline. Exemplary data supplied by the industries are displayed in Table 3. This table illustrates which current and voltage data at the three main points are explicitly specified at standard test conditions, such as irradiance of 1,000 w/m2 and temperature of $25°C$. Additional details of the parameters measured by the aforementioned equations are listed in Table 4.

Table 3. Electrical variables for photovoltaic (PV) cell under the standard test conditions.

variable	Kyocera KC200GT	Shell SQ85	Shell ST40
Kind	Polycrystalline	Monocrystalline	Thin film
Open circuit voltage, V_{OC} (volt)	32.9	22.20	23.30
Short circuit current, I_{Sc} (amp)	8.21	5.45	2.68
Voltage at maximum power, V_{MPP}(volt)	26.3	16.60	17.20
Current at maximum power, I_{MPP}(amp)	7.61	4.95	2.41
Temperature coefficient of V_{OC}, $K_{V,OC}$	-0.123	-0.0725	-0.1, $(volt/\circ c)$
Temperature coefficient of I_{SC}, $K_{I,SC}$	3.18×10^{-10}	0.8×10^{-3}	0.35×10^{-3}, $(volt/\circ c)$
Number of cells in series, N_C	54	36	36

Results of the single diode model

Every group of the optimal variables was estimated by several runs led to zero error at the three main I-V points. There were three types of SCs: Polycrystalline cell Kyocera KC200GT, monocrystalline cell Shell SQ85, and thin film ST40. The run of each type is presented in this subsection. Table 5 presents the optimal parameters of the SDM for the polycrystalline cell Kyocera KC200GT using the IEO. Table 5

Table 4. Input variables to the improved equilibrium optimizer (IEO) algorithm.

Parameters	SDM	DDM
Dimension of problem, d	3	5
Initial population size, N_{pini}	50	80
Maximum no. of fitness evaluations, NFE_{max}	50.000	60.000
The range of parameters $[X_{min}, X_{max}]$	$a = [0.1, 2.0]$ $R_s = [0.0001, 1]$ ohm $R_p = [40, 200]$ ohm	$a_1 = [0.1, 2.0]$ $a_2 = [0.1, 2.0]$ $I_{o1} = [10^{-12}, 10^{-6}]$ amp $R_s = [0.0001, 1]$ ohm $R_p = [40, 200]$ ohm

210 also presents the accuracy of the IEO in generating the PV parameters. The results of the best run of the
211 monocrystalline PV cell (Shell SQ85) are presented in Table 6. Table 7 presents the results obtained by
the run of the thin-film PV cell (Shell ST40) using the IEO.

Table 5. Optimal variables estimated by the IEO for the single-diode model of polycrystalline, Kyocera KC200GT.

Run-No	Optimized parameters			Calculated parameters		Error
	a	R_S (ohm)	R_P (ohm)	I_O (amp)	I_{PV} (amp)	E
1	0.4105	0.0007	43.8390	3.07E-27	8.2101	0
2	0.3494	0.0010	43.8350	5.06E-32	8.2102	0
3	1.0464	0.0010	50.5571	1.37E-10	8.2102	$1.39E - 28$
4	1.1205	0.0010	53.4895	7.05E-10	8.2102	$9.66E - 26$
5	0.3712	0.0008	43.8341	3.91E-30	8.2102	0
6	1.3315	0.0449	78.0334	2.81E-08	8.2147	$6.53E - 27$
7	1.6246	0.0010	151.2808	9.62E-07	8.2101	0
8	0.4774	0.0010	43.8344	2.13E-23	8.2102	0
9	1.3325	0.0089	70.3248	2.84E-08	8.2110	$3.94E - 30$
10	0.3517	0.2152	43.6181	8.21E-32	8.2505	0
11	1.0185	0.0002	49.6954	6.93E-11	8.2100	0
12	0.4160	0.0753	43.7651	7.13E-27	8.2241	0
13	0.9492	0.0010	43.8343	1.07E-11	8.2102	0
14	1.2509	0.1403	95.3509	8.12E-09	8.2221	$7.59E - 25$
15	0.5229	0.0104	43.8229	2.37E-21	8.2119	0
16	1.4470	0.1103	181.9726	1.37E-07	8.2149	0
17	0.4153	0.0374	43.7961	6.38E-27	8.2170	0
18	0.4778	0.0004	43.8338	2.22E-23	8.2101	$3.16E - 30$
19	0.9559	0.0007	43.8341	1.30E-11	8.2101	$1.58E - 25$
20	0.7702	0.0010	44.9910	1.89E-14	8.2102	$7.61E - 28$
21	1.6672	0.0009	190.3722	1.45E-06	8.2100	0
22	1.6277	0.0009	153.5346	9.93E-07	8.2101	$2.84E - 29$
23	1.6750	0.0010	200.0000	1.56E-06	8.2100	$2.23E - 25$
24	1.1749	0.2297	135.4552	2.16E-09	8.2239	0
25	0.9312	0.0498	43.7842	6.33E-12	8.2193	$7.88E - 31$
26	0.8439	0.0009	45.8630	3.58E-13	8.2102	0
27	0.94361	0.0013	47.7275	9.17E-12	8.2102	0
28	1.6677	0.0008	193.4348	1.46E-06	8.2100	0
29	0.4168	0.1344	43.7342	7.98E-27	8.2352	0
30	1.2660	0.0709	74.3245	1.03E-08	8.2178	0

212
213   Tables (5,6,7) reveal a small difference in the values of series resistance R_S in both Kyocera KC200GT
214 and monocrystalline but thin film cell ST40 apparently show a wider spread due to the limited current
215 capability of the thin film cell. In addition, the comparison indicates that the value of R_S is nearly 1
216 for thin film and less than 0.4 for both multicrystalline and monocrystalline. The I-V curve is strongly
217 affected by the series resistance. According to the results, lower values of Rs lead the I–V characteristics
218 to move farther from the axis with respect to the maximum point, while higher values of Rs lead the
219 I–V characteristics to move closer to the axis as in fig. 5. This tendency occurs naturally with the IEO
220 parameter values.
221   The difference between I-V characteristics can be attributed not only to different values of R_S and
222 R_P, but also to ideality factor of the diode, a. It is demonstrated that the values of all variables change
223 significantly. However, every optimal solution can arrive at zero error for the three major points. All prior
224 studies displayed one I-V characteristic that passed across the three main points. However, a PV cell
225 characteristic was observed that is not normal when the designer concentrated on the three major points.
226 For each cell, there is an operating point on the characteristic in which the performance is greatest. These
227 points are referred as the major points. The algorithm arrived at the global optimal solution after 0.10
228 seconds with an error of zero value. This algorithm took less time to run compared to other metaheuristic
229 algorithms.
230   A scatter plot of the optimal values (30 points) of these three parameters is provided in Figs.(6, 7 and
231 8). It is showing that the value of each parameter changes significantly. This demonstrates that under
232 the same parameter values I_{PV}, I_O, a, R_S and R_P, the IEO algorithm has the highest efficiency for the

Table 6. Optimal variables estimated by the IEO for the single-diode model of monocrystalline photovoltaic cell, Shell SQ85.

Run-No	Optimized parameters			Calculated parameters		Error
	a	R_S (ohm)	R_P (ohm)	I_O (amp)	I_{PV} (amp)	E
1	0.4952	0.0010	42.4047	5.19E-23	5.1979	0
2	1.9999	0.0248	142.2184	1.08E-05	5.3762	0
3	1.9975	0.0478	179.6755	1.07E-05	5.3926	0
4	2.0000	0.0381	162.6624	1.09E-05	5.3861	0
5	2.0000	0.0546	200.00	1.09E-05	5.3987	0
6	2.0000	0.0009	115.7362	1.08E-05	5.3576	$7.88E-31$
7	1.1357	0.0031	45.5716	4.76E-10	5.2158	0
8	1.9955	0.0010	113.9509	1.04E-05	5.3562	0
9	2.0000	0.0010	115.7355	1.07E-05	5.3576	0
10	0.5286	0.1510	41.3043	1.48E-21	5.2209	0
11	1.9986	0.0010	115.1735	1.07E-05	5.3572	$1.55E-28$
12	0.3220	0.0010	42.4010	2.26E-35	5.1978	0
13	2.0000	0.0010	115.7355	1.08E-05	5.3576	0
14	2.0000	0.0009	115.7381	1.08E-05	5.3576	0
15	1.6533	0.2203	200.00	7.02E-07	5.4055	0
16	2.0000	0.0009	115.7466	1.08E-05	5.3576	0
17	0.2549	0.1756	40.2245	1.12E-44	5.2198	0
18	2.0000	0.0546	200.00	1.09E-05	5.3987	0
19	2.0000	0.0010	115.7355	1.08E-05	5.3576	0
20	1.9986	0.0010	115.1901	1.07E-05	5.3572	0
21	1.9999	0.0546	199.8438	1.09E-05	5.3987	0
22	0.3164	0.0514	41.3486	5.44E-36	5.2014	$1.16E-26$
23	2.0000	0.0009	115.7405	1.08E-05	5.3576	0
24	1.6864	0.0010	58.2724	9.08E-07	5.2665	0
25	0.4776	0.1820	40.2556	7.38E-24	5.2213	0
26	1.9928	0.0010	112.8824	1.03E-05	5.3553	0
27	1.8995	0.0389	107.3014	5.37E-06	5.3533	0
28	0.2306	0.0010	40.4010	2.23E-49	5.1854	0
29	2.0000	0.0010	115.7355	1.08E-05	5.3576	0
30	0.8333	0.0478	41.0522	1.09E-13	5.1989	0

Table 7. Optimal variables for the single-diode model of thin-film photovoltaic cell, Shell ST40.

Run-No	Optimized parameters			Calculated parameters		Error
	a	R_S (ohm)	R_P (ohm)	I_O (amp)	I_{PV} (amp)	E
1	0.3722	0.0009	61.4825	1.90E-32	2.6800	0
2	2.0000	0.0055	80.7240	2.56E-06	2.6802	0
3	0.4832	0.1381	61.3438	4.47E-25	2.6860	0
4	1.8316	0.3748	86.4215	7.32E-07	2.6916	$1.97E-31$
5	2.0000	0.7718	200.00	2.75E-06	2.6910	0
6	2.0000	0.0010	80.5100	2.56E-06	2.6800	0
7	0.6324	1.0000	60.8257	3.06E-19	2.7241	0
8	2.0000	0.7718	200.00	2.75E-06	2.6903	0
9	0.2588	0.2059	61.2756	1.69E-46	2.6890	0
10	0.1561	0.6689	60.8125	7.74E-77	2.7095	0
11	2.0000	0.0085	80.8260	2.56E-06	2.6803	0
12	1.0287	0.3286	62.2278	5.72E-12	2.6942	0
13	1.9993	0.1227	85.1764	2.56E-06	2.6839	0
14	0.1848	0.8890	60.5925	5.42E-65	2.7193	$1.51E-24$
15	2.0000	0.6067	135.2353	2.69E-06	2.6920	0
16	1.0079	0.0010	61.8808	3.27E-12	2.6800	0
17	2.0000	0.5032	116.1444	2.66E-06	2.6916	0
18	2.0000	0.3980	103.5123	2.64E-06	2.6903	$7.88E-31$
19	2.0000	0.0010	80.5112	2.56E-06	2.6800	0
20	2.0000	0.7127	168.6513	2.73E-06	2.6913	$1.37E-24$
21	2.0000	0.4524	109.4282	2.65E-06	2.6911	0
22	2.0000	0.0009	80.5115	2.56E-06	2.6800	0
23	0.4069	0.0009	61.4825	1.03E-29	2.6800	0
24	0.1303	0.5279	60.9536	5.18E-92	2.7032	0
25	0.6593	0.5741	60.9933	1.79E-18	2.7052	$8.27E-25$
26	0.4683	0.0021	61.4795	7.28E-26	2.6801	$4.43E-29$
27	0.2947	0.3023	61.1791	6.99E-41	2.6932	0
28	0.9640	0.0308	61.7630	9.44E-13	2.6813	$1.50E-26$
29	0.2048	0.5737	60.9078	1.14E-58	2.7052	0
30	0.4355	0.5503	60.9320	8.85E-28	2.7042	0

experimental I–V data for every module.

As displayed in the previous figures, every curve passes through the three known points. A plot of the optimal solutions are presented in Fig. 9. A difference in (a) is present approximately between 0.2 and 1.7, while that of (R_p) is approximately between 80 and 175 ohms.

Results of the double diode model

Using the same parameter values I_{ph}, I_{o1}, I_{o2}, a_1, a_2, R_S, and R_P, IEO is more consistent with the experimental I-V data of all types of modules. The estimation of the parameters of SCs based on the DDM has high precision, and the optimization of parameters is implemented for the DDM of different types. Five parameters are optimized for the DDM (a_1, a_2, R_S, R_P, I_{O1}), while two sustainable parameters
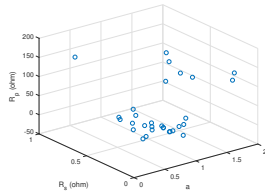
Figure 6. Scatter plot of the optimal values (30 sets) for the single-diode model of polycrystalline cell KC200GT.
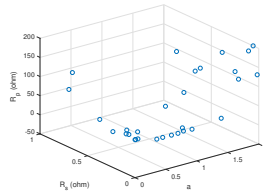
Figure 7. Scatter plot of the optimal values for the single-diode model of monocrystalline cell SQ85.
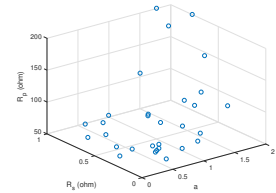
Figure 8. Scatter plot of the optimal values for the single-diode model of thin-film cell ST40.

are calculated (I_{O2}, I_{PV}) for their relation with the optimized parameters. The optimized parameters in various runs of the IEO algorithm for the DDM polycrystalline, KC200GT cell are listed in Table 8, SQ85 monocrystalline dish are listed in Table 9 and thin cells, shell ST40 are displayed in Table 10. For the

Table 8. Optimal variables for the double-diode model of polycrystalline photovoltaic cell, Kyocera KC200GT.

Run-No	Optimized Parameters					Calculated Parameters		Error
	a_1	a_2	R_S (ohm)	R_P (ohm)	I_{O1} (amp)	I_{O2}(amp)	I_{PV} (amp)	E
1	2.0000	1.5233	0.14386	67.3361	1.16E-07	3.21E-07	8.2275	0
2	1.8289	1.4930	0.2968	199.7722	1.00E-12	2.38E-07	8.2222	$1.02E-29$
3	2.0000	1.9995	0.0158	131.1378	1.00E-06	1.80E-05	8.2109	0
4	1.9915	1.2460	0.2805	61.5366	1.00E-12	7.34E-09	8.2474	0
5	1.9999	2.0000	0.0010	117.3639	1.00E-06	1.79E-05	8.2101	0
6	1.8059	1.5498	0.0010	50.0000	2.15E-07	4.013E-07	8.2102	0
7	1.9687	1.6440	0.0010	55.3115	1.00E-12	1.11E-06	8.2101	0
8	1.6413	2.0000	0.0012	117.0978	6.92E-09	1.89E-05	8.2101	0
9	2.0000	1.4957	0.0412	50.0000	1.00E-12	2.31E-07	8.2168	0
10	1.9717	1.9995	0.0010	117.1425	3.52E-09	1.89E-05	8.2101	0
11	2.0000	0.9102	0.4325	53.7084	4.62E-07	3.34E-12	8.2761	$1.26E-29$
12	1.6973	1.1087	0.2937	50.0000	2.34E-09	5.51E-10	8.2582	0
13	1.9769	2.0000	0.0027	118.7968	1.51E-12	1.90E-05	8.2102	0
14	2.0000	1.0519	0.3943	61.4608	1.00E-12	1.59E-10	8.2627	$7.61E-28$
15	1.8233	1.5153	0.0049	50.0000	1.00E-06	2.32E-07	8.2108	0
16	1.9087	1.5505	0.0010	50.0000	2.73E-07	4.13E-07	8.2102	$7.89-31$
17	1.5751	2.0000	0.0141	129.5679	1.00E-12	1.91E-05	8.2109	0
18	1.9727	1.2646	0.1699	50.0000	1.00E-06	9.14E-09	8.2379	0
19	2.0000	2.0000	0.0012	117.5239	9.77E-07	1.80E-05	8.2101	0
20	1.9745	1.9999	0.0327	153.4717	1.00E-12	1.91E-05	8.2117	0
21	1.9170	2.0000	0.0010	117.3639	1.00E-12	1.89E-05	8.2101	$7.13E-28$
22	1.9999	1.5504	0.0012	50.0000	3.68E-07	4.15E-07	8.2102	0
23	1.9920	2.0000	0.0010	117.3640	1.00E-12	1.89E-05	8.2101	0
24	1.6250	1.4812	0.2960	200.0000	1.90E-07	1.67E-07	8.2222	0
25	1.5044	1.3441	0.1288	50.5678	9.34E-08	2.08E-08	8.2309	0
26	1.3900	1.9999	0.0010	117.3636	1.00E-12	1.89E-05	8.2101	0
27	1.9999	2.0000	0.0010	117.3639	7.48E-09	1.89E-05	8.2101	0
28	2.0000	1.9947	0.0320	148.5751	2.98E-09	1.85E-05	8.2118	0
29	1.9904	1.5530	0.0034	50.0000	1.39E-08	4.36E-07	8.2106	$3.15E-30$
30	1.9982	0.5695	0.6635	55.6877	1.53E-09	1.41E-19	8.3078	$7.88E-31$

SDM, the optimized parameters resulted in zero error at the three main points. The 30 I-V plots resulting from various combinations of the variables are presented in Fig. 9. A plot of the optimal solution is presented in Fig. 10. All the curves passed through the open circuit, short circuit, and maximum power points. To easily analyze the optimized variables, standardized parameter values are presented in a parallel coordinate graph in Fig. 11. The value of R_P differs widely. However, I_{O1} ranges from approximately $0.01 p.u$ to $0.9 p.u$. The final value of the diode saturation current is very low, with an average of only several microamperes μA.

To summarize, regardless of the type of the PV cell or the PV parameter extraction model used, we cannot obtain one I-V characteristic with details of short circuits, maximum power, and open circuit points. Three point optimizations can reveal various characteristics in several tests. Section 5 confirms the effectiveness of the IEO algorithm in estimating the parameters of the SC, taking into account the SDM and DDM. The SDM used three types of PV modules to estimate the parameters of the PV model.

6 RESULTS OF COMPARING THE EFFECENCY OF THE IEO WITH OTHER METAHEURISTIC ALGORITHMS

The results of SC parameter estimation are compared with the results of other metaheuristic algorithms to evaluate the efficiency of applying the IEO algorithm.

Table 9. Optimal variables for the double-diode model of monocrystalline Shell SQ85.

Run-No	Optimized parameters					Calculated parameters			Error
	a_1	a_2	R_S (ohm)	R_P (ohm)	I_{O1} (amp)	I_{O2}(amp)	I_{PV} (amp)		E
1	2.0000	1.3534	0.1210	50.0000	7.84E-07	1.82E-08	5.4632	0
2	2.0000	2.0000	0.0010	117.3655	1.00E-12	1.08E-05	5.4500	0
3	2.0000	1.5570	0.0010	50.0000	1.00E-12	2.47E-07	5.4501	0
4	2.0000	1.7412	0.0261	69.0104	4.49E-07	1.43E-06	5.4521	0
5	1.9727	2.0000	0.0010	117.0170	8.39E-07	9.76E-06	5.4500	0
6	1.9675	2.0000	0.0010	117.3639	1.00E-12	1.08E-05	5.4500	$7.88E-31$
7	2.0000	1.5394	0.0010	50.0000	1.00E-06	1.84E-07	5.4501	0
8	1.8821	2.0000	0.0010	114.3371	9.90E-07	8.51E-06	5.4500	0
9	1.7597	1.9999	0.0056	119.4022	1.22E-07	1.00E-05	5.4503	0
10	1.7776	0.6201	0.5195	50.0000	5.62E-07	1.64E-18	5.5066	$3.16E-28$
11	1.9716	1.8592	0.0010	80.0694	1.00E-06	3.48E-06	5.4501	0
12	1.5348	1.5560	0.0016	50.0000	1.05E-12	2.44E-07	5.4502	0
13	1.9755	1.2397	0.2009	50.0005	3.33E-07	3.21E-09	5.4719	0
14	1.9170	2.0000	0.0010	117.3642	1.00E-12	1.08E-05	5.4500	0
15	1.8099	1.2020	0.4245	158.2137	1.00E-12	1.82E-09	5.4646	0
16	1.5581	1.5565	0.0010	50.0000	3.09E-07	5.85E-08	5.4501	0
17	1.9975	0.5000	0.6887	50.0000	1.00E-12	8.92E-23	5.5251	0
18	1.7492	2.0000	0.0010	117.3639	1.00E-12	1.08E-05	5.4500	$6.19E-25$
19	1.9707	2.0000	0.0013	117.5777	1.00E-12	1.08E-05	5.4501	0
20	1.9769	2.0000	0.0237	140.7349	1.33E-07	1.07E-05	5.4509	0
21	1.8546	1.6003	0.2212	145.2258	2.37E-07	3.87E-07	5.4583	$7.88E-31$
22	1.8666	1.2806	0.2578	66.6718	8.05E-07	5.39E-09	5.4711	0
23	1.7608	1.9859	0.0023	112.7487	1.00E-12	9.80E-06	5.4501	0
24	2.0000	2.0000	0.0010	117.3639	3.79E-07	1.04E-05	5.4500	0
25	2.0000	2.0000	0.0546	200.0000	1.00E-06	9.93E-06	5.4515	$1.97E-29$
26	1.9668	1.9200	0.0095	96.2587	5.21E-07	5.82E-06	5.4505	0
27	1.8934	2.0000	0.0037	119.6661	3.89E-09	1.08E-05	5.4502	0
28	1.9697	1.9996	0.0010	116.9501	5.45E-07	1.01E-05	5.4500	$4.65E-25$
29	2.0000	2.0000	0.0010	117.3639	1.03E-12	1.08E-05	5.4500	0
30	1.9478	1.5355	0.0010	50.0000	1.00E-06	1.68E-07	5.4501	0

Table 10. Optimal variables for the double-diode model of thin-film photovoltaic cell, Shell ST40.

Run-No	Optimized parameters					Calculated parameters			Error
	a_1	a_2	R_S (ohm)	R_P (ohm)	I_{O1} (amp)	I_{O2}(amp)	I_{PV} (amp)		E
1	1.9497	0.8051	0.0010	61.5456	1.00E-12	3.39E-15	2.6800	0
2	2.0000	1.9998	0.7719	199.9620	1.00E-06	1.75E-06	2.6904	$7.96E-29$
3	2.0000	0.6828	0.1757	61.7124	1.68E-07	6.97E-18	2.6876	0
4	2.0000	1.7425	1.0000	200.0000	1.00E-06	2.30E-07	2.6934	0
5	1.9999	0.8567	0.0518	61.5676	3.69E-09	2.65E-14	2.6823	0
6	1.9495	2.0000	0.2125	89.6850	1.00E-12	2.59E-06	2.6864	0
7	1.7032	0.5000	0.4038	64.0517	1.79E-07	6.46E-25	2.6969	0
8	1.6443	1.5964	0.4139	75.9185	2.32E-07	6.12E-08	2.6946	$1.84E-25$
9	1.9999	0.5185	0.0010	63.3347	1.00E-06	1.28E-23	2.6800	0
10	1.9396	2.0000	0.7815	199.6071	1.00E-06	1.22E-06	2.6905	$1.77E-30$
11	2.0000	0.5958	0.5694	63.31576	6.10E-07	1.60E-20	2.7041	$4.20-27$
12	1.8235	0.5501	1.0000	60.5959	1.00E-12	4.59E-22	2.7242	0
13	1.9419	0.5000	0.8368	60.6656	1.00E-12	3.05E-24	2.7169	0
14	1.9999	0.5000	0.0010	63.3348	1.00E-06	1.80E-24	2.6800	0
15	1.7237	0.5000	0.7316	60.7619	1.00E-12	3.05E-24	2.7123	0
16	1.7183	0.6149	1.0000	62.3562	4.42E-08	7.48E-20	2.7229	0
17	1.7775	2.0000	0.8158	200.0000	3.65E-07	7.10E-07	2.6909	$3.86E-29$
18	1.8125	1.6049	0.9979	132.9710	3.09E-07	4.81E-08	2.7001	0
19	1.4287	0.5322	0.7106	71.8892	4.00E-08	2.46E-22	2.7065	$1.13E-28$
20	1.9741	0.5007	0.0049	62.6031	5.44E-07	2.40E-24	2.6802	0
21	1.9138	1.9787	0.7749	188.6456	1.21E-09	2.37E-06	2.6910	$1.77E-30$
22	2.0000	0.5000	0.2572	61.2253	1.00E-12	3.02E-24	2.6913	0
23	1.9783	0.7001	0.0021	61.4963	1.01E-12	2.02E-17	2.6801	0
24	2.0000	0.5000	1.0000	60.5306	1.00E-12	3.06E-24	2.7242	0
25	1.9991	0.5000	0.4302	61.0538	1.00E-12	3.03E-24	2.6989	0
26	1.4757	0.7693	0.0010	61.5234	1.06E-12	6.90E-16	2.6800	0
27	1.9429	1.3129	0.6557	71.6179	3.02E-07	1.57E-09	2.7045	0
28	1.9632	2.0000	0.0010	80.3427	8.82E-07	1.42E-06	2.6800	0
29	2.0000	0.5000	0.1255	62.7184	6.31E-07	2.26E-24	2.6854	0
30	1.7438	0.5000	0.1682	63.5249	2.48E-07	7.51E-25	2.6871	0

The single diode model

This subsection presents a comparison between the solutions generated by the IEO algorithm and other algorithms that have been applied under the same conditions. The optimal error values obtained by the IEO was zero, as presented in Table 11. The IEO achieves the best results among all the six algorithms tested, followed by SCA, while the GA achieves the poorest results.

The double diode model

This subsection provides a comparison between the solutions generated by the IEO algorithm and other algorithms for the DDM. Table 12 indicates that the best error values obtained by the IEO were zero. The IEO thus achieved the best results of the six algorithms tested, followed by SCA. Whereas, GA achieved the poorest results. To sum up the obtained results, Tables 11 and 12 indicate that PSO produces
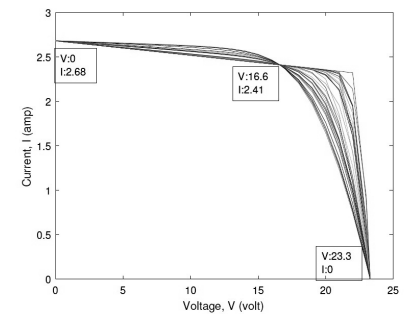
Figure 9. Plot of the optimal solutions for the single-diode model of thin-film cell ST40.
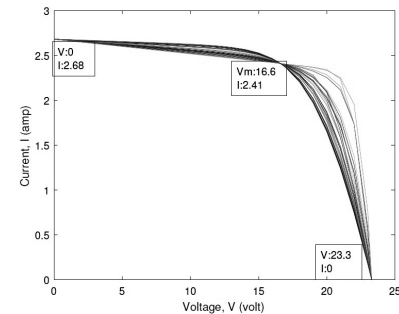
Figure 10. Plot of the optimal solutions for the double-diode model of thin film ST40.

Table 11. Comparison of various algorithms and IEO for the single-diode model.

Method	$I_{ph}(A)$	I_O	a	R_S	R_P	Error	Average	Std
GA Ismail et al. (2013)	0.7619	0.8087	1.5751	0.0299	52.3729	0.01908	0.07834	0.92E-03
PSO Wei et al. (2011a)	8.2305	3.09E-10	1.0802	0.2422	96.8938	0.0069	0.0059	3.48E-05
WOA Oliva et al. (2017a)	8.2255	8.05E-11	1.022	0.3253	172.4225	8.50E-15	4.17E-16	1.78E-15
GWO Rodríguez and Murillo (2017)	8.2109	5.78E-22	0.5084	0.005	43.8802	9.23E-10	2.29E-11	5.49E-11
SCA Chen et al. (2019)	8.2685	5.04E-27	0.4137	0.3130	43.894	6.66E-14	1.73E-09	2.44E-09
MVO Ali et al. (2016)	8.2106	1.25E-08	1.279	0.00524	64.3523	1.02E-07	3.91E-10	1.70E-09
EO	8.2133	2.23E-08	1.3159	0.0292	72.1747	1.81E-23	5.52E-17	3.02E-16
IEO	**8.2178**	**1.02E-08**	**1.2660**	**0.0709**	**74.3245**	**0**	**3.46E-29**	**1.89E-28**

Table 12. Comparison of the results of various algorithms and the IEO for the double-diode model.

Method	$I_{ph}(A)$	I_{O1}	I_{O2}	a_1	a_2	R_S	R_P	Error	Avg	Std
GA Ismail et al. (2013)	0.8207	3.47E-09	1.13E-09	1.38	1.15	0.2633	92.64	0.0670	0.065	0.009
PSO Wei et al. (2011a)	4.2023	2.04E-09	1.17E-10	1.21	1.07	0.17804	104.36	0.0075	0.006	8.9E-04
WOA Oliva et al. (2017a)	8.2125	3.41E-07	2.79E-11	1.82	0.99	0.0152	50.24	2.23E-14	1.2E-15	3.9E-15
GWO Rodríguez and Murillo (2017)	8.2325	6.15E-07	1.08E-12	2	0.88	0.1416	51.58	1.08E-11	7.9E-10	4.2E-09
SCA Chen et al. (2019)	8.2101	1.42E-12	7.19E-06	1.22	1.67	0.0042	200	2.78E-08	4.5E-09	1.1E-08
MVO Ali et al. (2016)	8.2122	4.04E-07	3.97E-07	2	1.54	0.0403	149.29	1.77E-10	1.2E-09	3.1E-09
EO	8.2153	5.53E-07	3.16E-08	1.95	1.43	0.0964	149.7943	5.28E-21	4.5E-18	2.4E-17
IEO	**8.2108**	**1.00E-06**	**2.32E-07**	**1.82**	**1.52**	**0.0049**	**50**	**0**	**2.8E-22**	**1.5E-21**
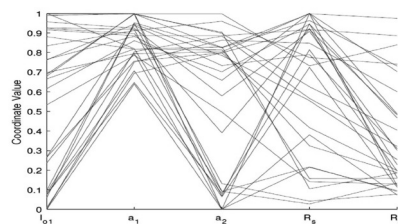
Figure 11. Parallel coordinate plot of the optimal solutions for the double-diode model of thin-film ST40.
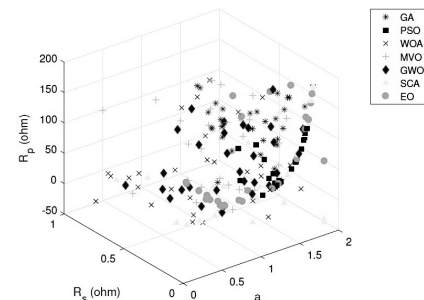
Figure 12. Scatter plot of the optimal results for the single-diode model of KC200GT cell using different algorithms.

better results than GA. In addition, GWO generates fewer errors than PSO, GA, WOA, SCA, and MVO. However, the IEO results are superior to those of all other approaches. Fig. 12 presents a comparison between the optimal results for the SDM of the KC200GT cell using different methods.

7 CONCLUSIONS AND FUTURE WORK

Developing an accurate model of the PV system is an important and challenging task. To obtain an accurate model, it is necessary to determine the optimal parameters for the PV model using an effective

optimization technique. The IEO algorithm is a recent optimization technique that is used for parameter extraction of the PV modules for the SDM and DDM. The IEO algorithm has various advantages, such as solution accuracy, convergence speed, and balance between analysis and exploitation. In this paper, the PV generator is modeled using the SDM and DDM, and the parameters of each model were optimally determined using the IEO algorithm. The IEO has been compared to the following six metaheuristic algorithms: GA, PSO, SCA, WOA, MVO, and GWO. The results achieved using the IEO are more accurate than those achieved by the other methods. The IEO could be a good candidate for solving the optimization problem of the SC systems. In future work, the IEO can be applied to identify the PV parameters for the multi-dimension diode and multi-diode models. Moreover, it can also be used for calculating the current-voltage characteristic of the multi-diode models.

CONFLICT OF INTEREST

The authors declare that there is no conflict of interest.

REFERENCES

AbdElminaam, D. S., Said, M., and Houssein, E. H. (2021). Turbulent flow of water-based optimization using new objective function for parameter extraction of six photovoltaic models. *IEEE Access*.

Alam, D., Yousri, D., and Eteiba, M. (2015a). Flower pollination algorithm based solar pv parameter estimation. *Energy Conversion and Management*, 101:410–422.

Alam, D., Yousri, D., and Eteiba, M. (2015b). Flower pollination algorithm based solar pv parameter estimation. *Energy Conversion and Management*, 101:410–422.

AlHajri, M., El-Naggar, K., AlRashidi, M., and Al-Othman, A. (2012). Optimal extraction of solar cell parameters using pattern search. *Renewable Energy*, 44:238–245.

Ali, E., El-Hameed, M., El-Fergany, A., and El-Arini, M. (2016). Parameter extraction of photovoltaic generating units using multi-verse optimizer. *Sustainable Energy Technologies and Assessments*, 17:68–76.

AlRashidi, M., AlHajri, M., El-Naggar, K., and Al-Othman, A. (2011). A new estimation approach for determining the i–v characteristics of solar cells. *Solar Energy*, 85(7):1543–1550.

Askarzadeh, A. and Rezazadeh, A. (2012). Parameter identification for solar cell models using harmony search-based algorithms. *Solar Energy*, 86(11):3241–3249.

Askarzadeh, A. and Rezazadeh, A. (2013a). Artificial bee swarm optimization algorithm for parameters identification of solar cell models. *Applied Energy*, 102:943–949.

Askarzadeh, A. and Rezazadeh, A. (2013b). Artificial bee swarm optimization algorithm for parameters identification of solar cell models. *Applied Energy*, 102:943–949.

Askarzadeh, A. and Rezazadeh, A. (2013c). Extraction of maximum power point in solar cells using bird mating optimizer-based parameters identification approach. *Solar energy*, 90:123–133.

Bagher, A. M., Vahid, M., Mohsen, M., and Parvin, D. (2015). Hydroelectric energy advantages and disadvantages. *American Journal of Energy Science*, 2(2):17.

Biswas, P. P., Suganthan, P., Wu, G., and Amaratunga, G. A. (2019). Parameter estimation of solar cells using datasheet information with the application of an adaptive differential evolution algorithm. *Renewable energy*, 132:425–438.

Chan, D., Phillips, J., and Phang, J. (1986). A comparative study of extraction methods for solar cell model parameters. *Solid-State Electronics*, 29(3):329–337.

Chellaswamy, C. and Ramesh, R. (2016). Parameter extraction of solar cell models based on adaptive differential evolution algorithm. *Renewable energy*, 97:823–837.

Chen, H., Jiao, S., Heidari, A. A., Wang, M., Chen, X., and Zhao, X. (2019). An opposition-based sine cosine approach with local search for parameter estimation of photovoltaic models. *Energy Conversion and Management*, 195:927–942.

Chin, C. S., Neelakantan, P., Yang, S. S., Chua, B. L., and Tze Kin Teo, K. (2011). Effect of partially shaded conditions on photovoltaic array's maximum power point tracking. *International Journal of Simulation–Systems, Science & Technology*, 12(3).

Dai, C., Chen, W., and Zhu, Y. (2009). Seeker optimization algorithm for digital iir filter design. *IEEE transactions on industrial electronics*, 57(5):1710–1718.

Derick, M., Rani, C., Rajesh, M., Farrag, M., Wang, Y., and Busawon, K. (2017). An improved optimization technique for estimation of solar photovoltaic parameters. *Solar Energy*, 157:116–124.

Diab, A. A. Z., Sultan, H. M., Do, T. D., Kamel, O. M., and Mossa, M. A. (2020). Coyote optimization algorithm for parameters estimation of various models of solar cells and pv modules. *IEEE Access*, 8:111102–111140.

Dunn, S. (2002). Hydrogen futures: toward a sustainable energy system. *International journal of hydrogen energy*, 27(3):235–264.

Easwarakhanthan, T., Bottin, J., Bouhouch, I., and Boutrit, C. (1986). Nonlinear minimization algorithm for determining the solar cell parameters with microcomputers. *International journal of solar energy*, 4(1):1–12.

Egbert, G. and Ray, R. (2000). Significant dissipation of tidal energy in the deep ocean inferred from satellite altimeter data. *Nature*, 405(6788):775.

El-Arini, M. M., Othman, A. M., and Fathy, A. (2013). A new optimization approach for maximizing the photovoltaic panel power based on genetic algorithm and lagrange multiplier algorithm. *International Journal of Photoenergy*, 2013.

El-Fergany, A. (2015). Efficient tool to characterize photovoltaic generating systems using mine blast algorithm. *Electric Power Components and Systems*, 43(8-10):890–901.

El-Naggar, K. M., AlRashidi, M., AlHajri, M., and Al-Othman, A. (2012a). Simulated annealing algorithm for photovoltaic parameters identification. *Solar Energy*, 86(1):266–274.

El-Naggar, K. M., AlRashidi, M., AlHajri, M., and Al-Othman, A. (2012b). Simulated annealing algorithm for photovoltaic parameters identification. *Solar Energy*, 86(1):266–274.

Faramarzi, A., Heidarinejad, M., Stephens, B., and Mirjalili, S. (2020). Equilibrium optimizer:anovel optimization algorithm. *Knowledge-Based System*, 191:105190.

Gao, X., Cui, Y., Hu, J., Xu, G., Wang, Z., Qu, J., and Wang, H. (2018a). Parameter extraction of solar cell models using improved shuffled complex evolution algorithm. *Energy conversion and management*, 157:460–479.

Gao, X., Cui, Y., Hu, J., Xu, G., Wang, Z., Qu, J., and Wang, H. (2018b). Parameter extraction of solar cell models using improved shuffled complex evolution algorithm. *Energy conversion and management*, 157:460–479.

Gong, W. and Cai, Z. (2013). Parameter extraction of solar cell models using repaired adaptive differential evolution. *Solar Energy*, 94:209–220.

Gotmare, A., Bhattacharjee, S. S., Patidar, R., and George, N. V. (2017). Swarm and evolutionary computing algorithms for system identification and filter design: A comprehensive review. *Swarm and Evolutionary Computation*, 32:68–84.

Hocaoğlu, F. O. (2011). Stochastic approach for daily solar radiation modeling. *Solar Energy*, 85(2):278–287.

Houssein, E. H. (2019). Machine learning and meta-heuristic algorithms for renewable energy: A systematic review. In *Advanced Control and Optimization Paradigms for Wind Energy Systems*, pages 165–187. Springer.

Humada, A. M., Hojabri, M., Mekhilef, S., and Hamada, H. M. (2016). Solar cell parameters extraction based on single and double-diode models: A review. *Renewable and Sustainable Energy Reviews*, 56:494–509.

Ismaeel, A. A., Houssein, E. H., Oliva, D., and Said, M. (2021). Gradient-based optimizer for parameter extraction in photovoltaic models. *IEEE Access*, 9:13403–13416.

Ismail, M. S., Moghavvemi, M., and Mahlia, T. (2013). Characterization of pv panel and global optimization of its model parameters using genetic algorithm. *Energy Conversion and Management*, 73:10–25.

Jacob, B., Balasubramanian, K., Azharuddin, S. M., Rajasekar, N., et al. (2015). Solar pv modelling and parameter extraction using artificial immune system. *Energy Procedia*, 75:331–336.

Kang, T., Yao, J., Jin, M., Yang, S., and Duong, T. (2018). A novel improved cuckoo search algorithm for parameter estimation of photovoltaic (pv) models. *Energies*, 11(5):1060.

Kumar, C., Raj, T. D., Premkumar, M., and Raj, T. D. (2020). A new stochastic slime mould optimization algorithm for the estimation of solar photovoltaic cell parameters. *Optik*, 223:165277.

Li, S., Gong, W., Yan, X., Hu, C., Bai, D., Wang, L., and Gao, L. (2019). Parameter extraction of photovoltaic models using an improved teaching-learning-based optimization. *Energy Conversion and*

383   *Management*, 186:293–305.

384   Lim, L. H. I., Ye, Z., Ye, J., Yang, D., and Du, H. (2015). A linear identification of diode models from
385   single *i–v* characteristics of pv panels. *IEEE Transactions on Industrial Electronics*, 62(7):4181–4193.

386   Lin, P., Cheng, S., Yeh, W., Chen, Z., and Wu, L. (2017a). Parameters extraction of solar cell models
387   using a modified simplified swarm optimization algorithm. *Solar Energy*, 144:594–603.

388   Lin, P., Cheng, S., Yeh, W., Chen, Z., and Wu, L. (2017b). Parameters extraction of solar cell models
389   using a modified simplified swarm optimization algorithm. *Solar Energy*, 144:594–603.

390   López, P. R., Jurado, F., Reyes, N. R., Galán, S. G., and Gómez, M. (2008). Particle swarm optimization for
391   biomass-fuelled systems with technical constraints. *Engineering Applications of Artificial Intelligence*,
392   21(8):1389–1396.

393   Mathew, D., Rani, C., Kumar, M. R., Wang, Y., Binns, R., and Busawon, K. (2017). Wind-driven
394   optimization technique for estimation of solar photovoltaic parameters. *IEEE Journal of Photovoltaics*,
395   8(1):248–256.

396   Munshi, A. A. and Yasser, A.-R. M. (2017). Comparisons among bat algorithms with various objective
397   functions on grouping photovoltaic power patterns. *Solar Energy*, 144:254–266.

398   Navabi, R., Abedi, S., Hosseinian, S. H., and Pal, R. (2015). On the fast convergence modeling and
399   accurate calculation of pv output energy for operation and planning studies. *Energy conversion and*
400   *management*, 89:497–506.

401   Oliva, D., Abd El Aziz, M., and Hassanien, A. E. (2017a). Parameter estimation of photovoltaic cells
402   using an improved chaotic whale optimization algorithm. *Applied Energy*, 200:141–154.

403   Oliva, D., El Aziz, M. A., and Hassanien, A. E. (2017b). Parameter estimation of photovoltaic cells using
404   an improved chaotic whale optimization algorithm. *Applied Energy*, 200:141–154.

405   Oliva, D., Elaziz, M. A., Elsheikh, A. H., and Ewees, A. A. (2019). A review on meta-heuristics methods
406   for estimating parameters of solar cells. *Journal of Power Sources*, page 126683.

407   Oliva, D., Ewees, A. A., Aziz, M. A. E., Hassanien, A. E., and Peréz-Cisneros, M. (2017c). A chaotic
408   improved artificial bee colony for parameter estimation of photovoltaic cells. *Energies*, 10(7):865.

409   Osama, S., Darwish, A., Houssein, E. H., Hassanien, A. E., Fahmy, A. A., and Mahrous, A. (2017). Long-
410   term wind speed prediction based on optimized support vector regression. In *2017 eighth international*
411   *conference on intelligent computing and information systems (ICICIS)*, pages 191–196. IEEE.

412   Osheba, D. S., Azazi, H. Z., and Shokralla, S. (2017). Parameter estimation of a photovoltaic array using
413   direct search optimization algorithm. *Journal of Renewable and Sustainable Energy*, 9(4):043501.

414   Park, J., Kim, H.-g., Cho, Y., and Shin, C. (2014). Simple modeling and simulation of photovoltaic panels
415   using matlab/simulink. *Advanced Science and Technology Letters*, 73:147–155.

416   Rodríguez, A. S. and Murillo, E. C. (2017). Automatic parametrization of support vector machines for
417   short texts polarity detection. *CLEI Electron. J.*, 20(1):6–1.

418   Salam, Z., Ishaque, K., and Taheri, H. (2010). An improved two-diode photovoltaic (pv) model for pv
419   system. In *2010 Joint International Conference on Power Electronics, Drives and Energy Systems &*
420   *2010 Power India*, pages 1–5. IEEE.

421   Siddiqui, M. and Abido, M. (2013). Parameter estimation for five-and seven-parameter photovoltaic
422   electrical models using evolutionary algorithms. *Applied soft computing*, 13(12):4608–4621.

423   Tizhoosh, H. R. (2005). Opposition-based learning: a new scheme for machine intelligence. In *Interna-*
424   *tional conference on computational intelligence for modelling, control and automation agents, web*
425   *technologies and internet commerce (CIMCA-IAWTIC'06)*, volume 1, pages 695–701. IEEE.

426   Wei, H., Cong, J., Lingyun, X., and Deyun, S. (2011a). Extracting solar cell model parameters based on
427   chaos particle swarm algorithm. In *2011 International Conference on Electric Information and Control*
428   *Engineering*, pages 398–402. IEEE.

429   Wei, H., Cong, J., Lingyun, X., and Deyun, S. (2011b). Extracting solar cell model parameters based on
430   chaos particle swarm algorithm. In *2011 International Conference on Electric Information and Control*
431   *Engineering*, pages 398–402. IEEE.

432   Wei, H., Cong, J., Lingyun, X., and Deyun, S. (2011c). Extracting solar cell model parameters based on
433   chaos particle swarm algorithm. In *2011 International Conference on Electric Information and Control*
434   *Engineering*, pages 398–402. IEEE.

435   Yuan, X., Xiang, Y., and He, Y. (2014). Parameter extraction of solar cell models using mutative-scale
436   parallel chaos optimization algorithm. *Solar Energy*, 108:238–251.